Arabian Journal of Chemistry (2022) **15**, 104113

King Saud University

Arabian Journal of Chemistry

www.ksu.edu.sa
www.sciencedirect.com

ORIGINAL ARTICLE

Facile synthesis of a novel nanocomposite for determination of mercury and copper ions in food and water samples

Asma S. Al-Wasidi [a], Huda S. AlSalem [a], Azaa F. Alshalawi [a], Ahmed M. Naglah [b], Ahmed Al-Anwar [c], Ehab A. Abdelrahman [d,*]

[a] *Department of Chemistry, College of Science, Princess Nourah Bint Abdulrahman University, P.O. Box 84428, Riyadh 11671, Saudi Arabia*
[b] *Department of Pharmaceutical Chemistry, College of Pharmacy, King Saud University, P.O. Box 2457, Riyadh 11451, Saudi Arabia*
[c] *Botany Department, Faculty of Science, Zagazig University, Zagazig 44519, Egypt*
[d] *Chemistry Department, Faculty of Science, Benha University, Benha 13518, Egypt*

Received 17 June 2022; accepted 6 July 2022
Available online 15 July 2022

KEYWORDS

Sodium aluminum silicate hydrate;
3-bromo-5-chlorosalicylaldehyde;
Nanocomposites;
Preconcentration;
Heavy metals

Abstract This paper describes the modification of sodium aluminum silicate hydrate by 3-bromo-5-chlorosalicylaldehyde to form a new composite. Furthermore, X-ray diffraction (XRD), Fourier-transform infrared spectroscopy (FT-IR), Transmission electron microscopy (TEM), CHN elemental analysis, Nitrogen gas sorption analyzer, and Scanning electron microscopy (SEM) tools were used for characterizing the synthesized composite. The XRD pattern of the synthesized composite shows a halo at $2\Theta = 25°$, confirming the destruction of the crystalline structure of the nanomaterial owing to the association with an organic substance. The synthesized composite was utilized for the removal and preconcentration of mercury and copper ions from water and food samples. The maximum adsorption capacity of the synthesized composite towards mercury and copper ions is 107.53 and 130.89 mg/g, respectively. In addition, the relative standard deviation was less than 3 %, showing excellent reproducibility. The dynamic analytical ranges are 0.8–380 μg/L and 1.00–550 μg/L for copper and mercury ions, respectively. The preconcentration factor is 10.

* Corresponding author.
E-mail addresses: dr.ehabsaleh@yahoo.com, ehab.abdelrahman@fsc.bu.edu.eg (E.A. Abdelrahman).
Peer review under responsibility of King Saud University.

Production and hosting by Elsevier

https://doi.org/10.1016/j.arabjc.2022.104113

1. Introduction

Copper is an essential nutrient for humans and can be found in a variety of foods. It is necessary for both plants and mammals. Copper, which is commonly present in drinking water, can produce nausea, vomiting, diarrhoea, and/or stomach pain if ingested in excess. Overconsumption of copper, such as in water or copper supplements, can result in severe illness, including kidney and liver damage (Lenka et al., 2021; Zhou et al., 2020; Zafar et al., 2020). Small levels of mercury can create severe health issues and constitute a threat to the infant and foetal development. Mercury is damaging to the digestive, nervous, and immune systems, in addition to the kidneys, lungs, eyes, and skin. Mercury can be converted into methylmercury by bacteria. Consequently, fish and shellfish accumulate methylmercury. Large predatory fish have high mercury levels because they consume smaller fish that have consumed mercury-containing plankton (Yu et al., 2016; Giraldo et al., 2020; Pirarath et al., 2021). A notable instance of mercury exposure significantly harming human health occurred in Minamata, Japan, from 1932 and 1968, when a factory producing acetic acid leaked waste fluids into Minamata Bay. The effluent contained excessive concentrations of methylmercury. Local and visiting fishermen's primary source of income was the bay's abundance of fish and shellfish. No one understood for many years that mercury-contaminated fish were causing a strange illness in the local populace and surrounding areas. At least fifty thousand people were impacted to some degree, with over two thousand confirmed cases of Minamata disease. In the 1950 s, extreme symptoms of Minamata disease were associated with paralysis, brain damage, psychosis, and incomprehensible speech (Abou Taleb et al., 2021). For the removal and preconcentration of toxic metal ions from aqueous media and industrial water discharges, a number of well-recognized conventional techniques are typically employed. Many of these processes are characterized by disadvantages such as slowness, high cost, high energy consumption, and the generation of toxic sludge (Bavel et al., 2020; Madrakian et al., 2014; Boulaiche et al., 2019). Owing to its relatively fast adsorption reaction, decreased operational requirements, and high metallic sorption activity, adsorption has generally been regarded as one of the most critical and efficient techniques for purifying water from a wide range of inorganic and organic pollutants (Abdelrahman et al., 2021; Abdelrahman et al., 2020; Abdelrahman and Hegazey, 2019; Abdelrahman and Hegazey, 2019). Recent adsorbents in this research field are frequently composed of low-cost chemicals, metal oxide composites, and polymeric materials. Metal ion preconcentration and removal from aqueous medium can be accomplished by a variety of methods. The batch equilibrium technique is one of several widely employed techniques for removing and preconcentrating heavy metals from their medium (Hao et al., 2022; Sunil et al., 2018). Nanomaterials and their composites, such as attapulgite-MnO_2 nanocomposite, attapulgite-Ag nanocomposite, C60-SESMP-Fe_3O_4 inorganic magnetizable nanocomposite, and saccharine-based carbonyl multi-walled carbon nanotubes, play an important role in life for their multiple applications such as hydrogen storage, colorizing antibacterial agent for pentalite emulsion paint, and removal of heavy metals (Allawi et al., 2022; Abdulkareem et al., 2022; Alheety et al., 2019; Majeed et al., 2020; Raoof Mahmood et al., 1294 (2019).; Alheety et al., 2022; Patel et al., 2020; Mishra et al., 2019; Mondal et al., 2019). Scientists are attempting to create inexpensive and simple materials from wastes (Asatkar et al., 2020). In addition, previous studies confirm that loading organic materials, such as 2,4-dihydroxybenzaldehyde, thioglycolic acid, 5-bromosalicylaldehyde, 1-hydroxy-2-acetonaphthone, and 4,6-diacetylresorcinol onto nanomaterials renders the resulting composites effective for removing heavy metals (Al-Wasidi et al., 2022; Gad et al., 2022; Khalifa et al., 2020). In this paper, sodium aluminum silicate hydrate was simply synthesized utilizing rice husk as a silicon source and waste aluminum cans as an aluminum source, as stated by Ehab et al (Abdelrahman et al., 2021). Besides, sodium aluminum silicate hydrate reacted with (3-aminopropyl)trimethoxysilane then modified by 3-bromo-5-chlorosalicylaldehyde utilizing microwave heating for creating a novel composite. The synthesized composite was characterized using XRD, FT-IR, TEM, CHN elemental analyzer, nitrogen gas sorption analyzer, and SEM. The synthesized composite was utilized for the removal and preconcentration of copper and mercury ions from aqueous media using the batch method.

2. Experimental

2.1. Chemicals

Sodium hydroxide (NaOH), (3-aminopropyl)trimethoxysilane ($C_6H_{17}NO_3Si$), hydrochloric acid (HCl), 3-bromo-5-chlorosalicylaldehyde ($C_7H5BrClO_2$), toluene (C_7H_8), ethanol (C_2H_6O), mercury(II) chloride ($HgCl_2$), copper(II) chloride dihydrate ($CuCl_2{\cdot}2H_2O$), nitric acid (HNO_3), potassium nitrate (KNO_3), thiourea (CH_4N_2S), and ethylenediaminetetraacetic acid disodium salt dihydrate ($C_{10}H_{18}N_2Na_2O_{10}$) were obtained from Sigma Aldrich Company and utilized without additional refining. The rice husk was obtained from a rice mill located near the Egyptian city of Zagazig. Besides, aluminum cans were obtained from a local market in Zagazig city, Egypt.

2.2. Synthesis of composite

Firstly, sodium aluminum silicate hydrate sample was synthesized as described by Ehab et al (Abdelrahman et al., 2021). The reaction between sodium aluminum silicate hydrate and (3-aminopropyl)trimethoxysilane was carried out as described by Khalifa et al but with slight modifications (Khalifa et al., 2020). 2 g of sodium aluminum silicate hydrate and 2.20 mL of (3-aminopropyl)trimethoxysilane was refluxed for 24 hrs using 50 mL of toluene. The obtained product was separated utilizing a centrifuge, washed with ethanol, and dried at 65 °C for 24 hrs. Besides, 1 g of sodium aluminum silicate hydrate/(3-aminopropyl)trimethoxysilane sample, 1 g of 3-bromo-5-chlorosalicylaldehyde, and 50 mL of ethanol were mixed then transferred to a 100 mL Teflon-lined stainless-steel autoclave for hydrothermal treatment at 120 °C for 3 hrs utilizing a microwave oven. The product was separated with a centrifuge, washed with ethanol, and then dried at 55 °C for 24 hrs. Scheme 1 represents the steps required for the modification of sodium aluminum silicate hydrate by 3-bromo-5-chlorosalicylaldehyde.

2.3. Instrumentation

X-ray diffraction pattern of the synthesized composite was obtained using a D8 Advance X-ray diffractometer. Infrared spectrum of the synthesized composite was obtained using a Bruker FT-IR spectrometer. The surface morphology of the synthesized composite was obtained using a JEOL 2000 scanning electron microscopy. The morphology of the synthesized composite was obtained using an EM-2100 high-resolution transmission electron microscopy. The percentages of CHN of the synthesized composite was obtained using a 2400 PerkinElmer CHN Elemental Analyzer. Utilizing a 210 Buck Scientific atomic absorption spectrometer with an acetylene–air flame, the concentration of copper and mercury ions was determined. The wavelengths for mercury and copper were 184.89 and 324.80 nm, respectively.

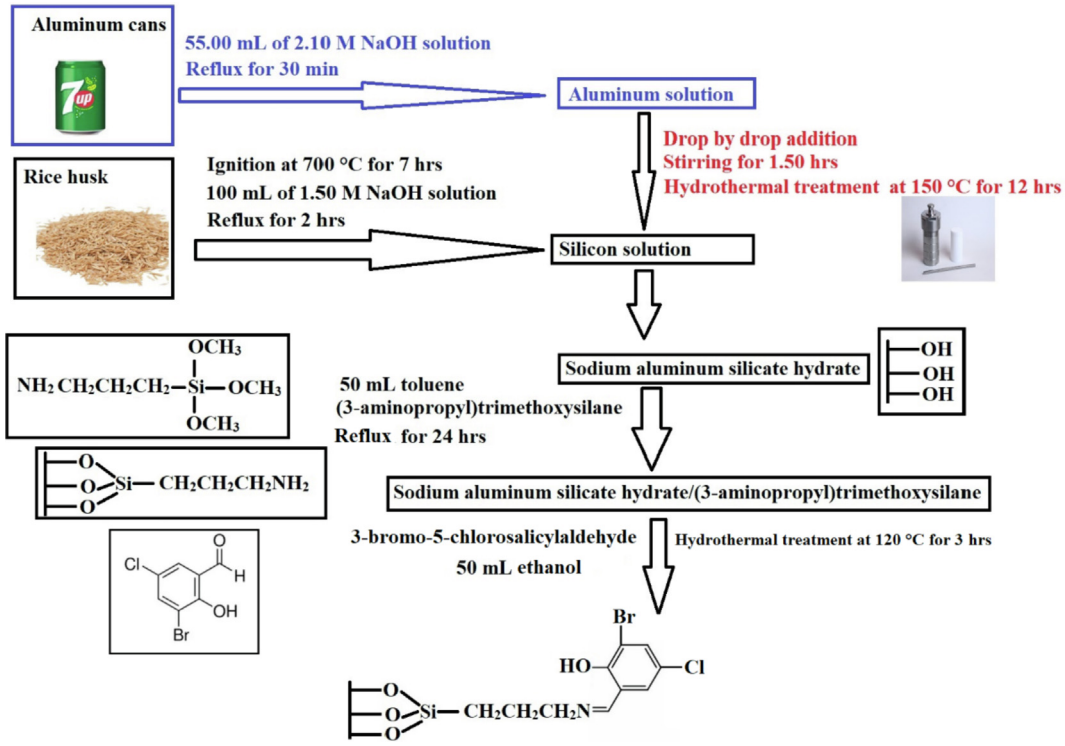

Scheme 1 Modification of sodium aluminum silicate hydrate by 3-bromo-5-chlorosalicylaldehyde.

2.4. Removal of mercury and copper ions from aqueous media

0.05 g of the synthesized composite was mixed with 50 mL of 150 mg/L of the copper or mercury solution at different pH (2–8) to investigate the effect of pH. After stirring the mixture for 3 hrs, the composite was separated using a centrifuge. Using an atomic absorption spectrometer, the final concentration of the copper or mercury ions in the filtrate was estimated. 0.1 M NaOH or HCl was used for modifying the pH. The effect of time was examined by mixing 0.05 g of the synthesized composite with 50 mL of 150 mg/L of the copper or mercury solution at pH = 6 for different times (5–120 min). After certain intervals of stirring, the composite was separated. Using an atomic absorption spectrometer, the final concentration of the copper or mercury ions in the filtrate was estimated. The effect of temperature was examined by mixing 0.05 g of the synthesized composite with 50 mL of 150 mg/L of the copper or mercury solution at pH = 6 and different temperatures (298–322 K). After 80 min of stirring, the composite was separated. Using an atomic absorption spectrometer, the final concentration of the copper or mercury ions in the filtrate was estimated. The effect of concentration was examined by mixing 0.05 g of the synthesized composite with 50 mL of different concentrations (5–200 mg/L) of the copper or mercury solution at a pH = 6. After 80 min of stirring, the composite was separated. Using an atomic absorption spectrometer, the final concentration of the copper or mercury ions in the filtrate was estimated. The amount of removed mercury or copper ions per gram of the composite (Q, mg/g) was determined using equation (1).

$$Q = [C_i - C_e] \times \frac{V}{M} \tag{1}$$

The percent removal (% R) of mercury or copper ions was determined using equation (2).

$$\%R = \frac{C_i - C_e}{C_i} \times 100 \tag{2}$$

C_i (mg/L) is the initial concentration of mercury or copper ions. C_e (mg/L) is the equilibrium concentration of mercury or copper ions in the filtrate. V (L) is the volume of mercury or copper solution. M (g) is the quantity of the composite. To assess the effect of desorption, 0.05 g of the synthesized composite was mixed for 80 min with 50 mL of 5 mg/L of the mercury or copper solution at a pH = 6. The composite was then separated using a centrifuge. Besides, the ions adsorbed on the synthesized composite were desorbed by shaking the loaded composite for 15 min with 5 mL of 0.5 M desorbing agents, such as thiourea, EDTA disodium salt, and nitric acid. The percentage of desorption (% D) was determined using equation (3).

$$\%D = \frac{100 C_d V_d}{(C_i - C_e)V} \tag{3}$$

The concentration of mercury or copper ions in the extractant is denoted by C_d (mg/L). Besides, V_d (L) is the volume of the extractant. To assess the reusability of the synthesized composite, five adsorption/desorption cycles utilizing nitric acid as a desorbing agent were performed in succession. After each run, the removal percentage (% R) was determined using equation (1). The method described by Khalifa et al (Altowayti et al., 2021) was used to determine the point of zero charge (pH_{PZC}) of the synthesized composite: Using 0.1 M hydrochloric acid or sodium hydroxide, the initial pH value of 50 mL of 0.025 M potassium nitrate solutions was adjusted to different

values (pH = 2–12). Besides, 0.10 g of the composite was added to each potassium nitrate solution, followed by 6 hrs of stirring. After separating the composite from the liquid phase, the final pH value (pH_{final}) of the filtrate was measured. The pH_{final} values were plotted versus the $pH_{initial}$ values. pH_{pzc} is the pH_{final} value at which a typical plateau is obtained (Altowayti et al., 2021).

2.5. Actual real sample collection and pretreatment

Several water samples were collected in polypropylene flasks previously cleaned with 10 % nitric acid. Before putting the samples in the refrigerator, 0.45 m membranes were used to filter them. In Benha City, Egypt, food samples (fish, spinach, and chicken) were acquired from a local market. Before each sample was sliced into little pieces, the edible component was extracted and cleaned with distilled water. After 12 hrs of drying at 60 °C, the samples were ground until uniform and then placed in polyethylene grabs. To expedite the procedure, microwave-assisted acid digestion was used to digest the materials. In separate Teflon digesting tubes, 0.5 g of dry sample was inserted, followed by the addition of 2 mL of 30 % hydrogen peroxide and 4 mL of nitric acid. After 15 min at room temperature, the tubes were hermetically sealed and heated using the one-step approach described below (power: 1650 W; temperature: 200 °C; ramp time: 16 min; cooling time: 16 min; hold time: 16 min). After bringing the test tubes to room temperature, nearly all of the solutions were evaporated and diluted with distilled water to 50 mL.

2.6. Preconcentration process

In a conical flask, 30 mL of digested solution or water sample was combined with 0.05 g of the synthesized composite. The pH of the mercury or copper solution was adjusted to 6.0 using sodium hydroxide and/or hydrochloric acid solutions, and the volume was increased to 50 mL using distilled water. In addition, the contents were stirred for 80 min before the adsorbent was separated and transferred to a 25 mL beaker. After adding 5 mL of 0.5 M nitric acid, the loaded composite was agitated for 10 min to allow the mercury or copper ions to desorb. Using an atomic absorption spectrometer, the concentration of mercury or copper ions in the filtrate was determined.

3. Results and discussion

3.1. Characterization of the synthesized composite

Fig. 1. A–B shows the X-ray diffraction patterns of sodium aluminum silicate hydrate and sodium aluminum silicate hydrate/3-bromo-5-chlorosalicylaldehyde composite, respectively (Abdelrahman et al., 2021). The sodium aluminum silicate hydrate peaks at 2Θ = 13.9°; 24.3°, 31.6°, 34.7°, 37.4°, 42.8°, 52.0°, 58.2°, 62.0°, and 63.9° correspond to lattice plans (110), (211), (310), (222), (321), (411), (510), (440), and (611), respectively as obtained from JCPDS No. 42–0216 (Abdelrahman et al., 2021). The XRD pattern of the sodium aluminum silicate hydrate/3-bromo-5-chlorosalicylaldehyde composite shows a halo at 2Θ = 25°, confirming the destruction of a crystalline structure of sodium aluminum silicate

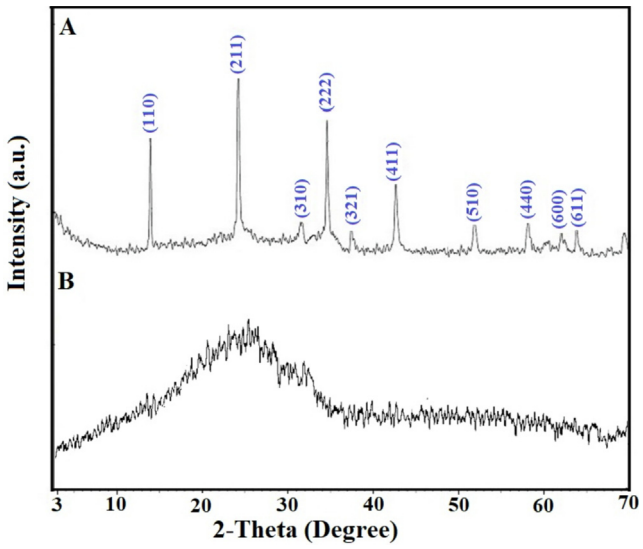

Fig. 1 The X-ray diffraction patterns of the sodium aluminum silicate hydrate (A) and sodium aluminum silicate hydrate/3-bromo-5-chlorosalicylaldehyde composite (B).

hydrate owing to the association of it with an amorphous background (Khalifa et al., 2020).

Fig. 2 shows the FT-IR spectrum of the sodium aluminum silicate hydrate/3-bromo-5-chlorosalicylaldehyde composite. The bands, which were observed at 3450 and 1650 cm^{-1}, are due to the stretching and bending vibration of OH and/or C = N, respectively. The bands, which were observed at 3085 and 3003 cm^{-1}, are due to the stretching vibration of aromatic and aliphatic CH, respectively. The bands, which were observed at 760 and 806 cm^{-1}, are due to the out of plane bending vibration of aromatic CH. The band, which was observed at 1348 cm^{-1}, is due to the bending vibration of CH. The bands, which were observed at 1496, 1552, and 1597 cm^{-1}, are due to the stretching vibration of aromatic C = C (Abdelrahman et al., 2021; Khalifa et al., 2020). Moreover, the bands, which were observed at 1450 and 1095 cm^{-1}, are due to the external and internal asymmetric stretching of Y-O-Y (Y = Si and/or Al), respectively. Also, the bands, which were observed at 695 and 645 cm^{-1}, are due to the external and internal symmetric stretching of Y-O-Y ((Y = Si and/or Al), respectively. Besides, the bands, which were observed at

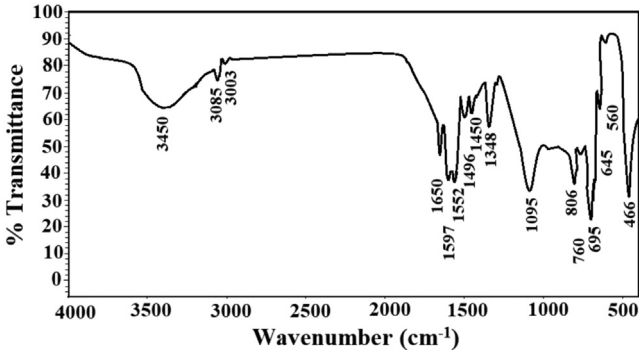

Fig. 2 The FT-IR spectrum of the sodium aluminum silicate hydrate/3-bromo-5-chlorosalicylaldehyde composite.

560 and 466 cm^{-1}, are due to the double ring vibration and bending vibration of Y-O-Y (Y = Si and/or Al), respectively (Abdelrahman et al., 2021; Khalifa et al., 2021).

The elemental analysis of the sodium aluminum silicate hydrate/3-bromo-5-chlorosalicylaldehyde composite shows carbon, hydrogen, and nitrogen content of 22.35 %, 2.94 %, and 2.07 %, respectively. The presence of carbon, nitrogen, and hydrogen in the composite is further proof that organic substance (composed of these components) was effectively loaded onto sodium aluminum silicate hydrate (Khalifa et al., 2020). The SEM and TEM investigations suggest that the composite's structure resembles that of cotton. As seen in Figs. 3 and 4, this indicates that the crystalline phase is associated with an amorphous background (Khalifa et al., 2020).

3.2. Removal of mercury and copper ions from aqueous media

3.2.1. Effect of pH

The influence of pH on the % R of mercury or copper ions and the adsorption capacity of the sodium aluminum silicate hydrate/3-bromo-5-chlorosalicylaldehyde composite are illustrated in Fig. 5A-B, respectively. If the pH is raised from 2 to 6, both the removal rate and adsorption capacity improve substantially. In addition, it has been demonstrated that a slight increase occurs when the pH changes from 6 to 8. Therefore, pH = 6 was chosen as the optimal pH for further tests. At pH = 6, the removal percentages of mercury and copper ions are 69.67 and 85.29 %, respectively. At pH = 6, the sodium aluminum silicate hydrate/3-bromo-5-chlorosalicylal dehyde composite has an adsorption capacity of 104.50 mg/g for mercury ions and 127.94 mg/g for copper ions. The pH_{final} versus $pH_{initial}$ curve for several potassium nitrate solutions is clarified in Fig. 5C to get the point of zero charge (pH_{PZC}) (Abdelrahman et al., 2021; Khalifa et al., 2020). Also, the results confirmed that the sodium aluminum silicate hydrate/3-bromo-5-chlorosalicylaldehyde composite point of zero charge is 3.18. It was found that when the pH of the mercury or copper solution is less than 3.18, the sodium aluminum silicate hydrate/3-bromo-5-chlorosalicylaldehyde composite has a positive charge owing to the presence of positive hydrogen ions which repelled the mercury or copper ions, resulting in a decrease in the removal percentage and the adsorption capacity. Besides, when the pH of the mercury or copper solution is greater than 3.18, the sodium aluminum silicate hydrate/3-bromo-5-chlorosalicylaldehyde composite has a negative charge owing to the presence of negative hydroxide ions which are attracted to the mercury or copper ions and hence increase the removal percentage and the adsorption capacity (Khalifa et al., 2020).

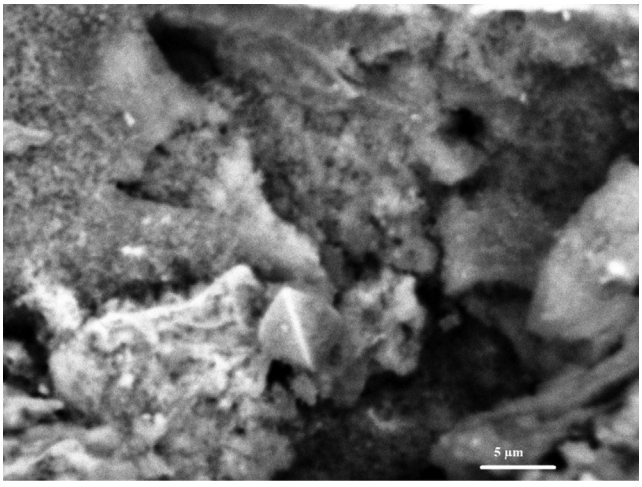

Fig. 3 The FE-SEM image of the sodium aluminum silicate hydrate/3-bromo-5-chlorosalicylaldehyde composite.

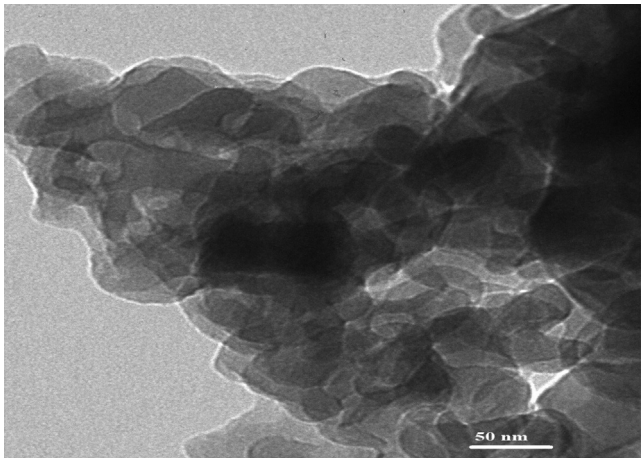

Fig. 4 The HR-M image of the sodium aluminum silicate hydrate/3-bromo-5-chlorosalicylaldehyde composite.

3.2.2. Effect of time

The influence of time on the percent removal of mercury or copper ions and the adsorption capacity of the sodium aluminum silicate hydrate/3-bromo-5-chlorosalicylaldehyde composite are illustrated in Fig. 6-B, respectively. If the time is raised from 5 to 80 min, both the removal rate and adsorption capacity improve immensely. In addition, it has been demonstrated that there is a slight increase when the time is raised from 80 to 120 min due to the saturation of active sites. As a result, time = 80 min was chosen as the optimal duration for future tests. At time = 80 min, the percent removal of mercury and copper ions is 70.67 and 86.00 %, respectively. At time = 80 min, the composite's adsorption capacities for mercury and copper ions are 106.0 and 129.0 mg/g, respectively.

Furthermore, two kinetic models were utilized to investigate the influence of contact time: pseudo-second-order (Equation (4)) and pseudo-first-order (Equation (5)) (Khalifa et al., 2020).

$$\frac{t}{Q_t} = \frac{1}{K_2 Q_e^2} + \frac{1}{Q_e} t \tag{4}$$

$$\log (Q_e - Q_t) = log Q_e - \frac{K_1}{2.303} t \tag{5}$$

Q_e (mg/g) is the equilibrium adsorption capacity of the synthesized composite. Q_t (mg/g) is the adsorption capacity of the synthesized composite towards the mercury or copper ions at contact time t. The rate constant of the pseudo-first-order model is denoted by K_1 (1/min), while the rate constant of the pseudo-second-order model is denoted by K_2 (g/mg.min). The pseudo-first-order and pseudo-second-order models are clarified in Fig. 7A-B, respectively. According to Table 1, the

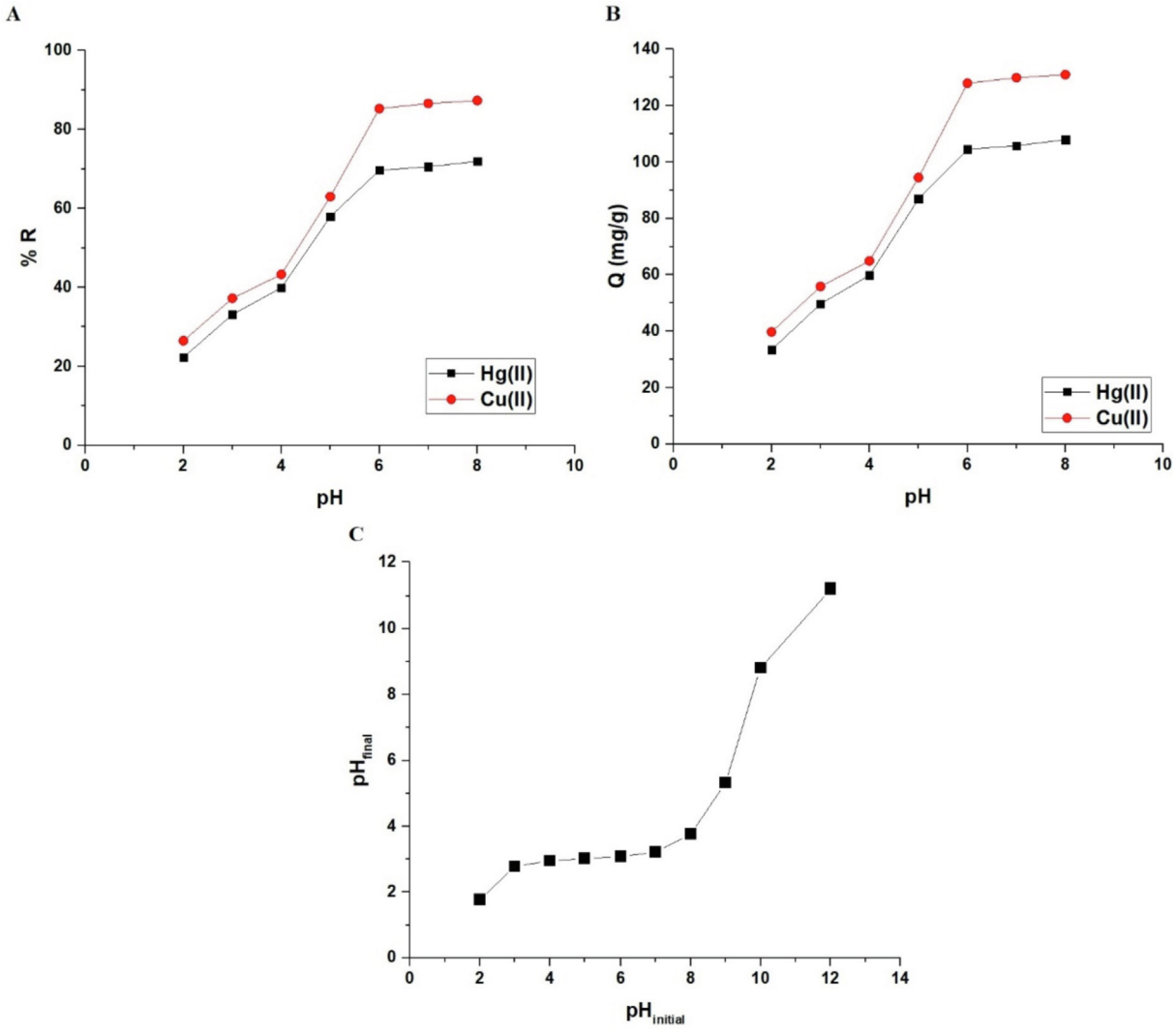

Fig. 5 The influence of pH of the mercury or copper solution on % removal (A) and adsorption capacity (B). The plot of pH_{final} versus $pH_{initial}$ (C).

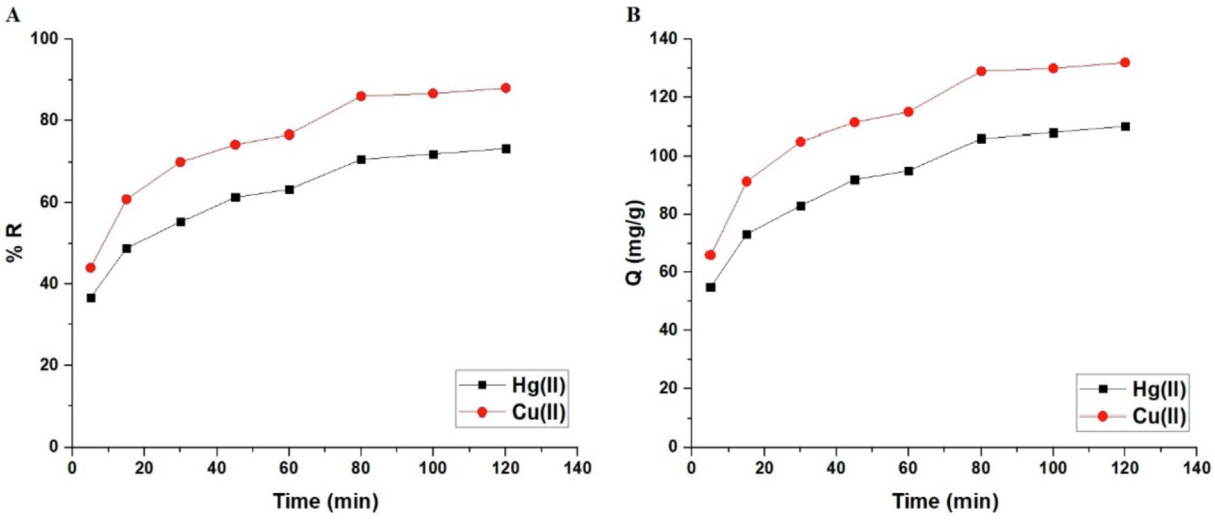

Fig. 6 The influence of contact time of the mercury or copper solution on % removal (A) and adsorption capacity (B).

correlation coefficients (R^2) of the pseudo-first-order model are less than those of the pseudo-second-order model. Moreover, the pseudo-second-order adsorption capacity is more in line with experimental adsorption capacity than the pseudo-first-order adsorption capacity. Consequently, the pseudo-second-order model provided a more accurate explanation for the kinetic data than the pseudo-first-order model. Thus, it appears that the chemical reaction is involved in the rate-controlling process (Khalifa et al., 2020). Nonlinear kinetic models were studied as described by Altowayti et al. (Figures omitted for brevity). The R^2 value derived from the nonlinear plot is much smaller than that derived from the linear model. The results of this study showed that the linear method is a good way to show the kinetic data (Altowayti et al., 2021).

3.2.3. Effect of temperature

The influence of temperature on the percent removal of mercury or copper ions and the adsorption capacity of the sodium aluminum silicate hydrate/3-bromo-5-chlorosalicylaldehyde composite are illustrated in Fig. 8A-B, respectively. If the temperature is raised from 298 to 328 K, both the removal percentage and adsorption capacity drop. Therefore, temperature = 298 K was chosen as the optimal temperature for the subsequent studies. The removal percentages of mercury and copper ions at 328 K are 29.83 and 52.97 %, respectively. At 328 K, the sodium aluminum silicate hydrate/3-bromo-5-chlorosalicylaldehyde composite had an adsorption capacity of 44.75 mg/g for mercury ions and 79.45 mg/g for copper ions. Utilizing equations (6) and (7), the thermodynamic parameters such as change in entropy (ΔS^o), change in enthalpy (ΔH^o), and change in free energy (ΔG^o) were calculated (Khalifa et al., 2020).

$$\ln K_d = \frac{\Delta S^o}{R} - \frac{\Delta H^o}{RT} \tag{6}$$

$$\Delta G^o = \Delta H^o - T\Delta S^o \tag{7}$$

T is the adsorption temperature (K) whereas K_d is the distribution constant (L/g). R is a gas constant (kJ/mol K). Utilizing equation (8), the distribution constant was determined (Khalifa et al., 2020).

$$K_d = \frac{Q_e}{C_e} \tag{8}$$

The plot of $\ln K_d$ versus temperature is illustrated in Fig. 8C. Table 2 is a listing of thermodynamic parameters. The fact that the enthalpy value exceeds 40 kJ/mol indicates that the adsorption of mercury or copper ions by the synthesized composite is chemical in nature as shown in Scheme 2 (Khalifa et al., 2020). Owing to the negative sign of enthalpy, the adsorption of mercury or copper ions is exothermic (Khalifa et al., 2020). Besides, owing to the negative sign of Gibbs free energy, the spontaneous adsorption of mercury or copper ions occurs when the synthesized composite is used. At the solution boundary/composite, the adsorption of mercury or copper ions occurs disorderly owing to the positive sign of entropy (Khalifa et al., 2020).

3.2.4. Effect of concentration

The influence of concentration on the percent removal of mercury or copper ions and the adsorption capacity of the sodium aluminum silicate hydrate/3-bromo-5-chlorosalicylaldehyde composite are illustrated in Fig. 9A-B, respectively. The percentage of mercury or copper ion removal reduces as the concentration rises from 5 to 200 mg/L, although the adsorption capacity rises (Khalifa et al., 2020).

Using Freundlich (Equation (9)) and Langmuir (Equation (10)) equilibrium isotherms, the concentration data were examined (Khalifa et al., 2020).

$$lnQ_e = lnK_F + \frac{1}{n} lnC_e \tag{9}$$

$$\frac{C_e}{Q_e} = \frac{1}{K_L Q_m} + \frac{C_e}{Q_m} \tag{10}$$

The maximum adsorption capacity of the sodium aluminum silicate hydrate/3-bromo-5-chlorosalicylaldehyde composite is denoted by Q_m (mg/g). The Langmuir constant is K_L (L/mg), while the Freundlich constant is K_F ((mg/g)(L/mg)$^{1/n}$). The heterogeneity constant is 1/n. Using equation (11), the Freundlich isotherm can be used to determine Q_m (Khalifa et al., 2020).

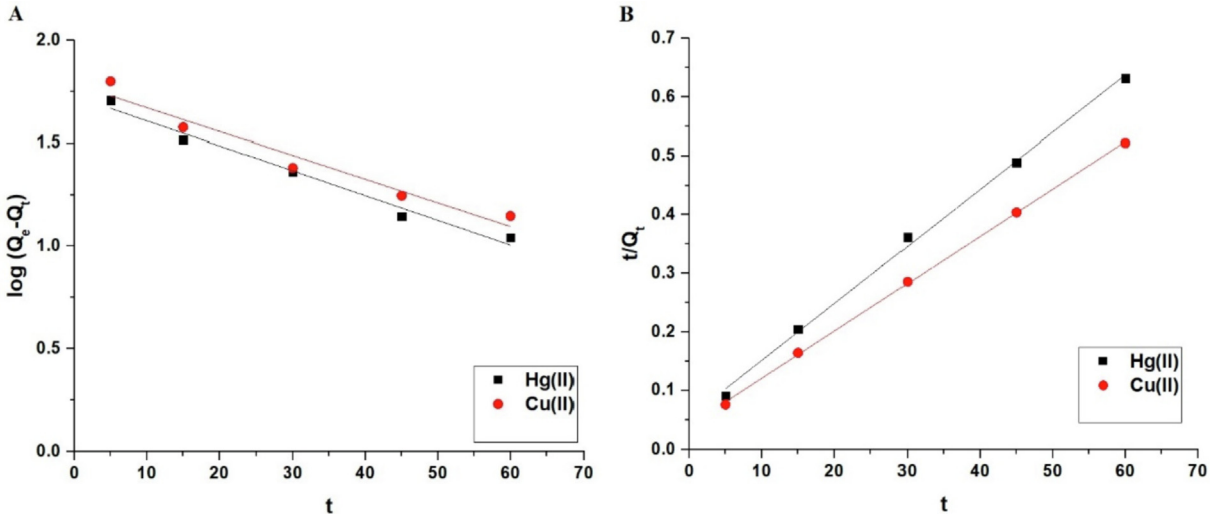

Fig. 7 The pseudo-first-order (A) and pseudo-second-order (B) kinetic models.

Table 1 Kinetic constants for the removal of mercury and copper ions using the sodium aluminum silicate hydrate/3-bromo-5-chlorosalicylaldehyde composite.

Metal ion	Pseudo first order				Pseudo second order			
	Q_e (mg/g)		K_1 (1/min)	R^2	Q_e (mg/g)		K_2 (g/mg.min)	R^2
	Calculated	Experimental			Calculated	Experimental		
Hg(II)	53.52	106.00	0.0278	0.9749	102.78	106.00	0.00175	0.9968
Cu(II)	61.22	129.00	0.0266	0.9363	123.92	129.00	0.0016	0.9995

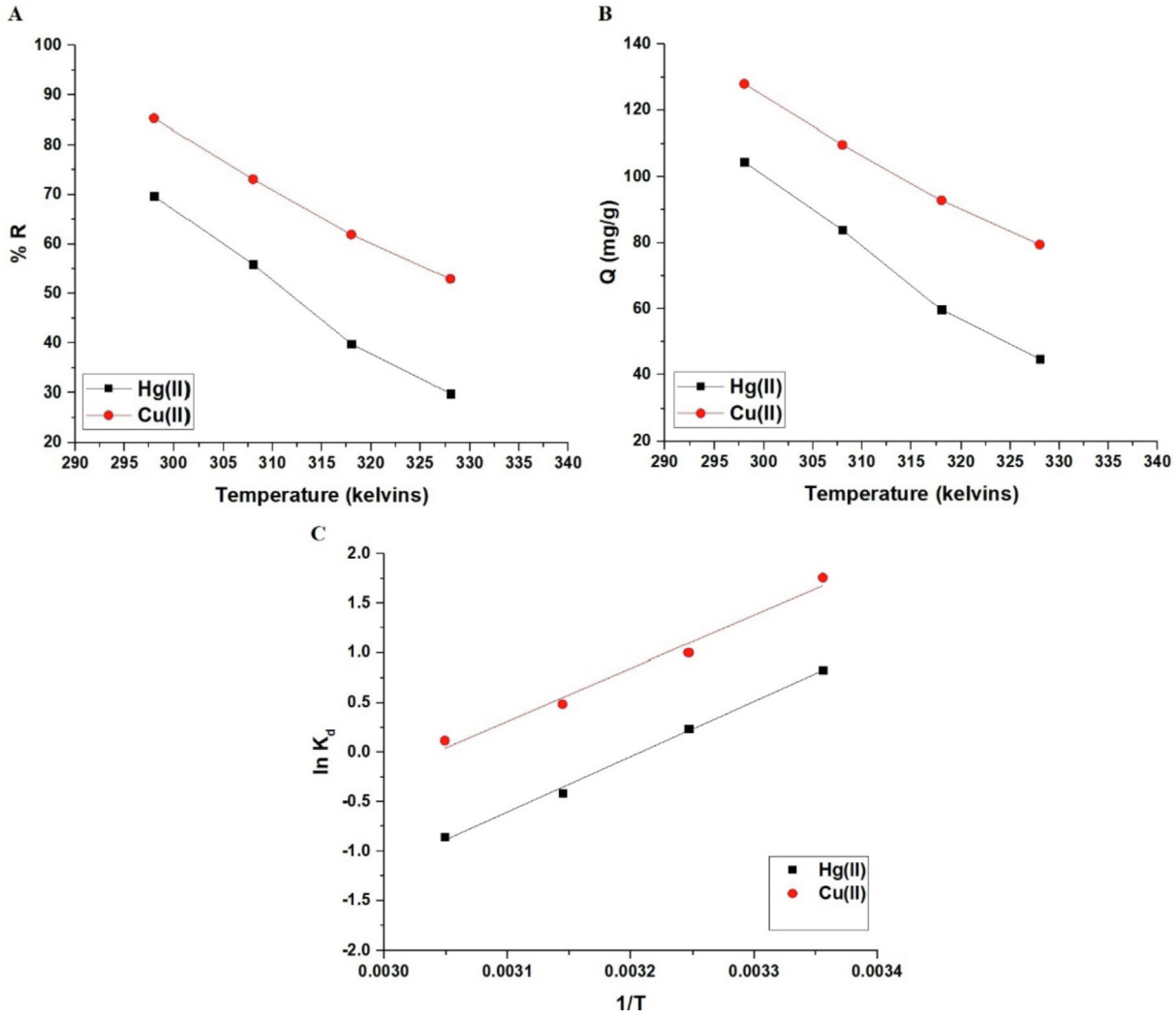

Fig. 8 The influence of temperature of the mercury or copper solution on % removal (A) and adsorption capacity (B). The plot of $\ln K_d$ versus temperature.

$$Q_m = K_F\left(C_i^{1/n}\right) \tag{11}$$

The Langmuir and Freundlich isotherms are clarified in Fig. 10A-B, respectively. According to Table 3, the Freundlich isotherm correlation coefficients (R^2) are smaller than Langmuir's. Consequently, the Langmuir isotherm represented equilibrium data more accurately than the Freundlich isotherm. The composite's maximal absorption capacity for mercury and copper ions is 107.53 and 130.89 mg/g, respectively. The maximum adsorption capacity of sodium aluminum silicate hydrate for mercury and copper ions is 60.34 and 85 mg/g, respectively. This confirms the effectiveness of the sodium aluminum silicate hydrate/3-bromo-5-chlorosalicylal dehyde composite owing to the ability of 3-bromo-5-chlorosalicylaldehyde to remove mercury or copper ions through the formation of chelates.

3.2.5. Effect of desorption and reusability

Fig. 11 illustrates the relationship between the amount of desorption and a few desorbing agents. Desorbing agents included

Table 2 Thermodynamic parameters for the removal of mercury and copper ions using the sodium aluminum silicate hydrate/3-bromo-5-chlorosalicylaldehyde composite.

Metal ion	ΔG^{o} (KJ/mol)				ΔS^{o} (KJ/molK)	ΔH^{o} (KJ/mol)
	Temperature (kelvin)					
	298	308	318	328		
Hg(II)	−91.36	−92.86	−94.35	−95.85	0.1498	−46.71
Cu(II)	−84.94	−86.29	−87.65	−89.00	0.1355	−44.56

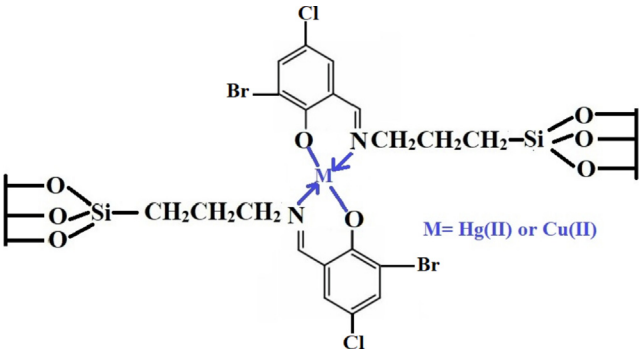

Scheme 2 Adsorption mechanism of mercury and copper ions onto the sodium aluminum silicate hydrate/3-bromo-5-chlorosalicylaldehyde composite.

EDTA disodium salt, thiourea, and nitric acid at a concentration of 0.5 M. Thiourea is bidentate ligand while EDTA is a hexadentate ligand forming highly stable complexes with metal ions in aqueous solution. So, they have the affinity to uptake studied metal ions from the sodium aluminum silicate hydrate/3-bromo-5-chlorosalicylaldehyde composite. Also, the use of nitric acid increases remarkably the concentration of hydrogen ion leading to desorption of studied metal ions from the sodium aluminum silicate hydrate/3-bromo-5-chloro salicylaldehyde composite due to the instability of the formed complexes at highly acidic solutions. The results reveal that 0.5 M nitric acid is the optimum desorbing agent for extracting the greatest quantity of investigated ions from the sodium aluminum silicate hydrate/3-bromo-5-chlorosalicylaldehyde composite. Furthermore, Fig. 12 illustrates the relationship between percent removal and cycle number. The small decrease in removal percentage shows that the sodium aluminum silicate hydrate/3-bromo-5-chlorosalicylaldehyde composite can be effectively regenerated and reused for the removal of mercury and copper ions from aqueous media.

3.2.6. *Effect of co-existing ions*

To examine the influence of various anions and cations on the extraction efficiency of mercury and copper ions using the present approach, the probable interfering ion was added to a 50 mL solution containing 200 μg/L of the studied metal ion at various concentrations. The extraction method was executed precisely as described previously, and its efficacy was tested. As the greatest concentration of the accompanying ion resulted in a 5 percent extraction error, the tolerance limit was established. Table 4 demonstrates that the majority of coexisting ions have a relatively high tolerance limit, indicating the technique's selectivity. Thus, the method is applicable to the examination of real samples containing several components.

3.3. *Application*

Prior to atomic absorption spectrometer examination, the proposed separation method was utilized to preconcentrate mercury and copper ions in real samples (sea water, river water,

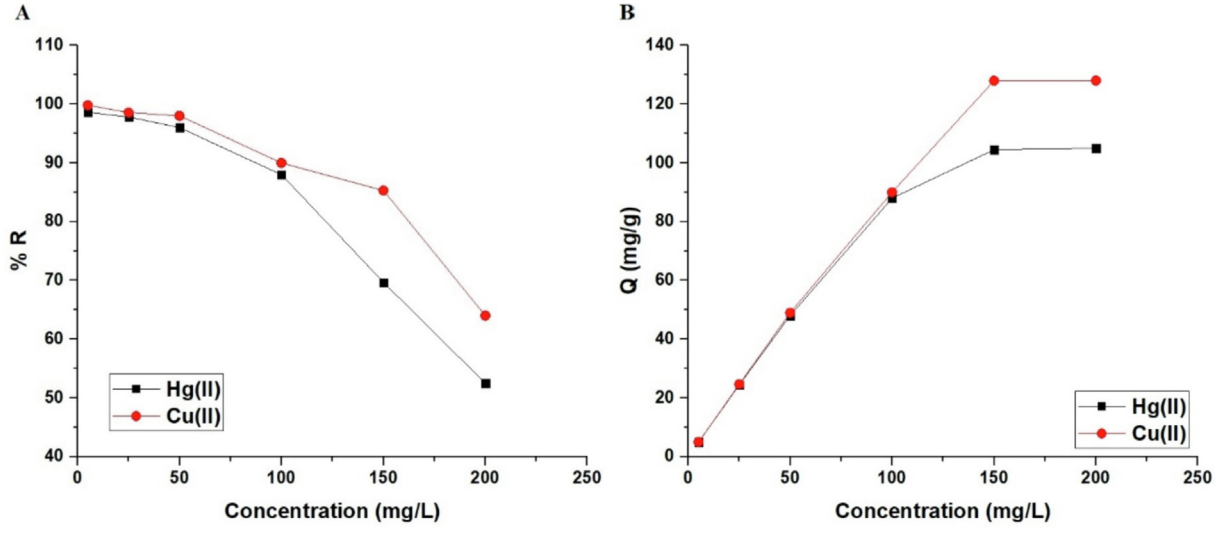

Fig. 9 The influence of concentration of the mercury or copper solution on % removal (A) and adsorption capacity (B).

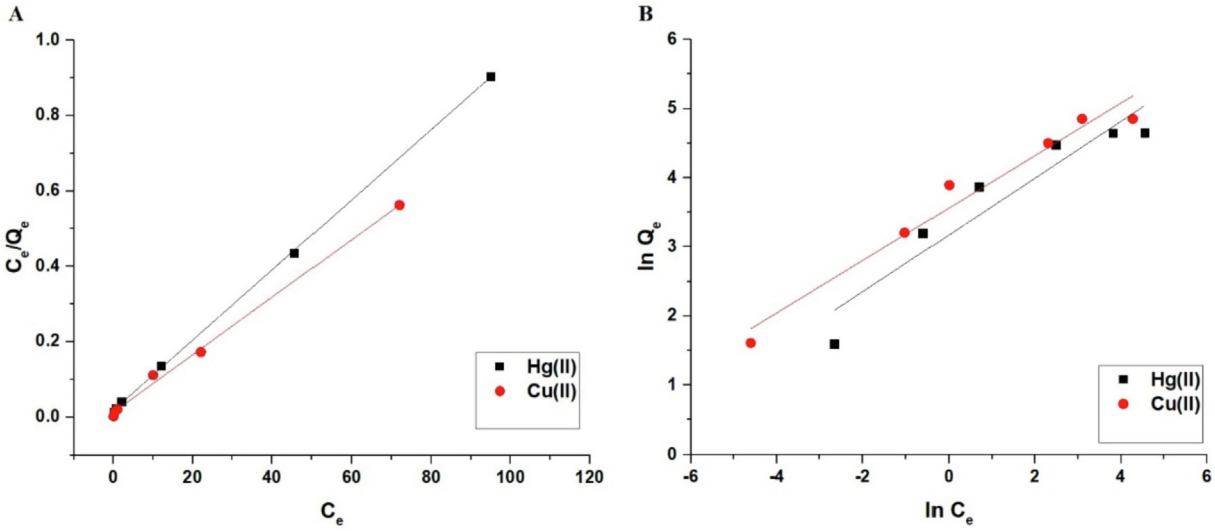

Fig. 10 The Langmuir (A) and Freundlich (B) isotherms.

Table 3 Equilibrium constants for the removal of mercury and copper ions using the sodium aluminum silicate hydrate/3-bromo-5-chlorosalicylaldehyde composite.

Metal ion	Langmuir			Freundlich		
	Q_m (mg/g)	K_L (L/mg)	R^2	Q_m (mg/g)	K_F (mg/g)(L/mg)$^{1/n}$	R^2
Hg(II)	107.53	0.4997	0.9997	186.93	23.88	0.8736
Cu(II)	130.89	0.5872	0.9967	235.97	35.23	0.9554

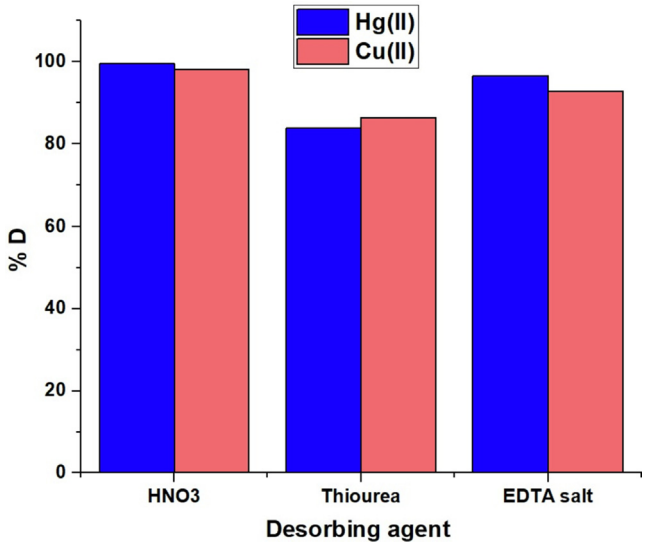

Fig. 11 The plot of % desorption versus several desorbing solutions.

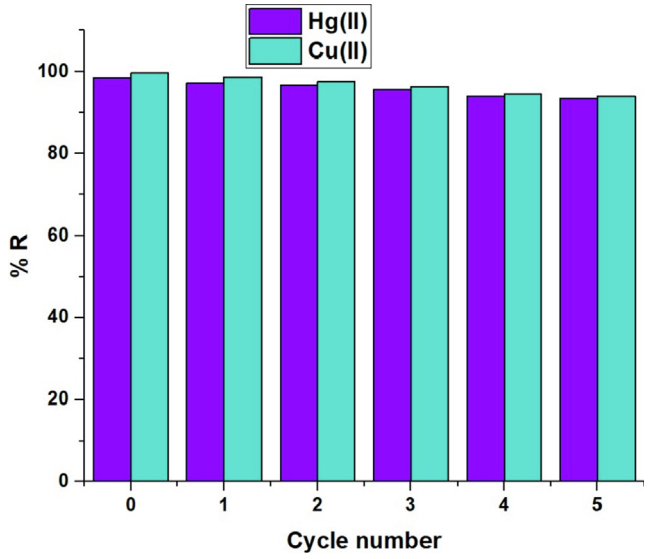

Fig. 12 The plot of % removal versus the cycle number.

fish muscles, spinach leaves, and chicken muscles). The findings of the preconcentration of mercury and copper ions, as well as the recoveries for the spiked samples, are summarized in tables 5 and 6, respectively. The recovery results indicate the process's precision, adaptability, and quantitative separation (greater than95%). In addition, the % RSD was less than 3.5%, showing excellent reproducibility. Standard solutions of each metal ion were processed at the optimum conditions to construct the calibration curves. The dynamic analytical ranges are 0.8–380 μg/L and 1.00–550 μg/L for copper and mercury ions, respectively. The preconcentration factor is 10.

Table 5 Determination of mercury ions in real samples.

Sample	Added volume from Hg(II) stock solution (1000 μg/L)								
	0 mL			0.2 mL			0.4 mL		
	Found concentration (μg/L)	% Recovery	% RSD	Found concentration (μg/L)	% Recovery	% RSD	Found concentration (μg/L)	% Recovery	% RSD
Sea water	0.294 ± 0.011	–	3.042	4.238 ± 0.177	99.091	3.364	8.094 ± 0.116	98.369	1.151
River water	0.244 ± 0.007	–	2.422	4.160 ± 0.112	98.422	2.177	8.142 ± 0.103	99.558	1.014
Chicken muscles	1.516 ± 0.059	–	3.149	5.490 ± 0.092	99.927	1.351	9.400 ± 0.132	99.571	1.128
Fish muscles	25.660 ± 1.052	–	3.302	29.490 ± 0.439	99.825	1.201	33.060 ± 0.885	99.003	2.156
Spinach leaves	2.880 ± 0.104	–	2.905	6.820 ± 0.254	99.524	3.005	10.680 ± 0.269	98.947	2.029

% RSD is the relative standard deviation. Found concentrations were represented as (mean ± (SD × t/$\sqrt{n}$), n (no of measurements) = 5, t (critical t value) = 2.776, Confidence level = 95 %. SD is standard deviation.

Table 6 Determination of copper ions in real samples.

Sample	Added volume from Cu(II) stock solution (1000 μg/L)								
	0 mL			0.2 mL			0.4 mL		
	Found concentration (μg/L)	% Recovery	% RSD	Found concentration (μg/L)	% Recovery	% RSD	Found concentration (μg/L)	% Recovery	% RSD
Sea water	4.606 ± 0.148	–	2.585	8.422 ± 0.210	98.253	2.012	12.480 ± 0.226	99.792	1.461
River water	9.010 ± 0.188	–	1.683	12.380 ± 0.143	95.538	0.929	16.520 ± 0.387	97.896	1.885
Chicken muscles	5.998 ± 0.109	–	1.474	9.560 ± 0.371	96.002	3.128	13.778 ± 0.103	99.216	0.604
Fish muscles	8.132 ± 0.105	–	1.038	12.070 ± 0.250	99.887	1.671	15.918 ± 0.322	99.463	1.628
Spinach leaves	6.950 ± 0.272	–	3.179	10.570 ± 0.173	97.449	1.321	14.708 ± 0.251	99.568	1.375

% RSD is the relative standard deviation. Found concentrations were represented as (mean ± (SD × t/$\sqrt{n}$), n (no of measurements) = 5, t (critical t value) = 2.776, Confidence level = 95 %. SD is standard deviation.

Table 4 Removal of mercury and copper ions from binary mixtures in the presence of several diverse ions.

Diverse ion	Tolerance limit (μg/L)	% R	
		Hg(II)	Cu(II)
Na(I)	1000	99.24	99.05
K(I)	1000	98.36	99.25
Ba(II)	90	95.87	96.14
Ca(II)	100	96.71	97.08
Mg(II)	100	97.54	96.54
Cd(II)	90	95.98	95.79
Fe(II)	80	97.80	96.46
Fe(III)	80	96.37	96.58
Zn(II)	100	97.54	97.05
Mn(II)	80	97.24	98.25
Ni(II)	100	96.96	95.74
Al(III)	90	98.63	97.47
Fe(III)	90	97.48	96.55
HCO^{3-}	1000	99.83	99.46
NO^{3-}	1000	99.92	99.22
Cl^{-}	1000	99.14	99.67
SO_4^{2-}	1000	99.48	99.77

4. Conclusions

In this study, sodium aluminum silicate hydrate was prepared then chemically modified by 3-bromo-5-chlorosalicylaldehyde. The synthesized composite was characterized using some physical and chemical instruments and was employed for the removal and preconcentration of mercury and copper ions from aqueous solutions and food samples (Sea water, river water, fish muscles, spinach leaves, and chicken muscles). The thermodynamic experiments revealed an exothermic, chemical, and spontaneous adsorption process. The synthesized composite has a maximum absorption capacity of 107.53 and 130.89 mg/g for mercury and copper ions, respectively.

Declaration of Competing Interest

The authors declare that they have no known competing financial interests or personal relationships that could have appeared to influence the work reported in this paper.

Acknowledgments

The authors are grateful to Princess Nourah Bint Abdulrahman University, Riyadh, Saudi Arabia for funding this work through Researchers Supporting Project number (PNURSP2022R35). Also, authors are grateful to King Saud University, Riyadh, Saudi Arabia for funding this work through Researchers Supporting Project number (RSP-2021/359).

References

Lenka, S.P., Shaikh, W.A., Owens, G., Padhye, L.P., Chakraborty, S., Bhattacharya, T., 2021. Removal of copper from water and wastewater using dolochar. Water. Air. Soil Pollut. 232, 167–180.

Zhou, H., Tan, Y., Gao, W., Zhang, Y., Yang, Y., 2020. Removal of copper ions from aqueous solution by a hydrotalcite-like absorbent FeMnMg-LDH. Water, Air, Soil Pollut. 231, 370–380.

Zafar, S., Khan, M.I., Lashari, M.H., Khraisheh, M., Almomani, F., Mirza, M.L., Khalid, N., 2020. Removal of copper ions from aqueous solution using NaOH-treated rice husk. Emerg. Mater. 3, 857–870.

Yu, J.G., Yue, B.Y., Wu, X.W., Liu, Q., Jiao, F.P., Jiang, X.Y., Chen, X.Q., 2016. Removal of mercury by adsorption: a review. Environ. Sci. Pollut. Res. 23, 5056–5076.

Giraldo, S., Robles, I., Ramirez, A., Flórez, E., Acelas, N., 2020. Mercury removal from wastewater using agroindustrial waste adsorbents. SN Appl. Sci. 2, 1–17.

Pirarath, R., Shivashanmugam, P., Syed, A., Elgorban, A.M., Anandan, S., Ashokkumar, M., 2021. Mercury removal from aqueous solution using petal-like MoS2 nanosheets. Front. Environ. Sci. Eng. 15, 1–10.

Abou Taleb, M.F., Albalwi, H., Abou El Fadl, F.I., 2021. Removal of mercury (II) from aqueous solution using silver nanocomposite: synthesis and adsorption mechanism. J. Inorg. Organomet. Polym. Mater. 31, 1825–1835.

Bavel, E., Afkhami, A., Madrakian, T., 2020. Removal and preconcentration of Pb(II) heavy metal ion from water and waste-water samples onto poly (vinyl alcohol)/polyethyleneimine/Fe3O4 microfibers nanocomposite. J. Polym. Environ. 28, 614–623.

Madrakian, T., Afkhami, A., Rezvani-Jalal, N., Ahmadi, M., 2014. Removal and preconcentration of lead(II), cadmium(II) and chromium(III) ions from wastewater samples using surface functionalized magnetite nanoparticles. J. Iran. Chem. Soc. 11, 489–498.

Boulaiche, W., Hamdi, B., Trari, M., 2019. Removal of heavy metals by chitin: equilibrium, kinetic and thermodynamic studies. Appl. Water Sci. 9, 1–10.

Abdelrahman, E.A., Abou El-Reash, Y.G., Youssef, H.M., Kotp, Y. H., Hegazey, R.M., 2021. Utilization of rice husk and waste aluminum cans for the synthesis of some nanosized zeolite, zeolite/zeolite, and geopolymer/zeolite products for the efficient removal of Co(II), Cu(II), and Zn(II) ions from aqueous media. J. Hazard. Mater. 401, 123813.

Abdelrahman, E.A., Alharbi, A., Subaihi, A., Hameed, A.M., Almutairi, M.A., Algethami, F.K., Youssef, H.M., 2020. Facile fabrication of novel analcime/sodium aluminum silicate hydrate and zeolite Y/faujasite mesoporous nanocomposites for efficient removal of Cu(II) and Pb(II) ions from aqueous media. J. Mater. Res. Technol. 9, 7900–7914.

Abdelrahman, E.A., Hegazey, R.M., 2019. Exploitation of Egyptian insecticide cans in the fabrication of Si/Fe nanostructures and their chitosan polymer composites for the removal of Ni(II), Cu(II), and Zn(II) ions from aqueous solutions. Compos. Part B Eng. 166, 382–400.

Abdelrahman, E.A., Hegazey, R.M., 2019. Utilization of waste aluminum cans in the fabrication of hydroxysodalite nanoparticles and their chitosan biopolymer composites for the removal of Ni(II) and Pb(II) ions from aqueous solutions: kinetic, equilibrium, and reusability studies. Microchem. J. 145, 18–25.

Hao, L., Li, L., Yu, S., Liu, J., 2022. Humic acid-coated hydrated ferric oxides-polymer nanocomposites for heavy metal removal in water. Sci. Total Environ. 834, 1–7.

Sunil, K., Karunakaran, G., Yadav, S., Padaki, M., Zadorozhnyy, V., Pai, R.K., 2018. Al-Ti2O6 a mixed metal oxide based composite membrane: a unique membrane for removal of heavy metals. Chem. Eng. J. 348, 678–684.

Allawi, A.H., Mohammed, M.Y., Ayrim, N.B., Alheety, M.A., Mahmood, A.R., 2022. Journal of the indian chemical society synthesis of attapulgite-MnO 2 nanocomposite from manganese complex by ultrasound for hydrogen storage. J. Indian Chem. Soc. 99, 100596.

Abdulkareem, M.A., Joudi, M.S., Ali, A.H., 2022. Eco-friendly synthesis of low-cost antibacterial agent (brown attapulgite-Ag nanocomposite) for environmental application. Chem. Data Collect. 37, 100814.

Alheety, M.A., Raoof, A., Al-Jibori, S.A., Karadağ, A., Khaleel, A.I., Akbaş, H., Uzun, O., 2019. Eco-friendly C60-SESMP-Fe3O4 inorganic magnetizable nanocomposite as high-performance adsorbent for magnetic removal of arsenic from crude oil and water samples. Mater. Chem. Phys. 231, 292–300.

Majeed, A.H., Hussain, D.H., Al-Tikrity, E.T.B., Alheety, M.A., 2020. Poly (o-Phenylenediamine-GO-TiO2) nanocomposite: modulation, characterization and thermodynamic calculations on its H2 storage capacity. Chem. Data Collect. 28, 100450.

Raoof Mahmood, A., Alheety, M.A., Asker, M.M.M., Zyaad Tareq, A., Karadağ, A., 1294 (2019).. Saccharine based carbonyl multi-walled carbon nanotubes: novel modification, characterization and its ability for removing Cd(II) and Cu(II) from soil and environmental water samples. J. Phys. Conf. Ser. https://doi.org/10.1088/1742-6596/1294/5/052003.

Alheety, M.A., Majeed, A.H., Ali, A.H., Mohammed, L.A., Destagul, A., Singh, P.K., 2022. Synthesis and characterization of eggshell membrane polymer-TiO2 nanocomposite for newly synthesized ionic liquid release. J. Iran. Chem. Soc. In Press. https://doi.org/10.1007/s13738-022-02584-x.

Patel, G., Raj Patel, A., Lambat, T.L., Mahmood, S.H., Banerjee, S., 2020. Rice husk derived nano-NiFe2O4@CAGC-catalyzed direct oxidation of toluene to benzyl benzoate under visible LED light. FlatChem. 21, 100163.

Mishra, R.K., Verma, K., Chaudhary, R.G., Lambat, T., Joseph, K., 2019. An efficient fabrication of polypropylene hybrid nanocomposites using carbon nanotubes and PET fibrils. Mater. Today Proc. 29, 794–800.

Mondal, A., Chouke, P.B., Sonkusre, V., Lambat, T., Abdala, A.A., Mondal, S., Chaudhary, R.G., 2019. Ni-doped ZnO nanocrystalline material for electrocatalytic oxygen reduction reaction. Mater. Today Proc. 29, 715–719.

Asatkar, A., Lambat, T.L., Mahmood, S., Mondal, A., Singh, M., Banerjee, S., 2020. Facile protocol for the synthesis of benzothiazole, benzoxazole and N-benzimidazole derivatives using rice husk derived chemically activated carbon. Mater. Today Proc. 29, 738–742.

Al-Wasidi, A.S., Naglah, A.M., Saad, F.A., Abdelrahman, E.A., 2022. Modification of silica nanoparticles with 4,6-diacetylresorcinol as a novel composite for the efficient removal of Pb(II), Cu(II), Co(II), and Ni(II) ions from aqueous media. J. Inorg. Organomet. Polym. Mater. In Press. https://doi.org/10.1007/s10904-022-02282-4.

Gad, H.M., El Rayes, S.M., Abdelrahman, E.A., 2022. Modification of silica nanoparticles by 2,4- dihydroxybenzaldehyde and 5-bromosalicylaldehyde as new nanocomposites for efficient removal and preconcentration of Cu(II) and Cd(II) ions from water, blood, and fish muscles. RSC Adv. 12, 19209–19224.

Khalifa, M.E., Abdelrahman, E.A., Hassanien, M.M., Ibrahim, W.A., 2020. Application of mesoporous silica nanoparticles modified with dibenzoylmethane as a novel composite for efficient removal of Cd (II), Hg(II), and Cu(II) ions from aqueous media. J. Inorg. Organomet. Polym. Mater. 30, 2182–2196.

Altowayti, W.A.H., Othman, N., Goh, P.S., Alshalif, A.F., Al-Gheethi, A.A., Algaifi, H.A., 2021. Application of a novel nanocomposites carbon nanotubes functionalized with mesoporous silica-nitrenium ions (CNT-MS-N) in nitrate removal: optimizations and nonlinear and linear regression analysis. Environ. Technol. Innov. 22,. https://doi.org/10.1016/j.eti.2021.101428 101428.